Physics and Applications of Mesoscopic Structures

P. Omling, N. Carlsson, K. Deppert, B. Kowalski,
H. Linke, M. S. Miller, P. Ramvall, L. Samuelson and W. Seifert
Department of Solid State Physics, University of Lund
Box 118, S-221 00 Lund, Sweden

Received July 21, 1995

The behaviour of electrons in certain quantum confined systems is described. The topics are the effective spin-splitting factors in two-dimensional structures, the exchange interaction of excitons confined in InAs/GaAs quantum dot systems, the magnetoresistance of 2D- and 1D-channels where the ballistic electron motion is perturbed by randomly deposited aerosol lead- particles, and on a 1D switching device, the Y-branch switch, where mode evolution rather than quantum interference effects are used.

I. Introduction

There is a large interest in understanding the physics of artificial quantum confined systems[1]. Today such objects can readily be manufactured in different semiconductors where the small effective masses make the quantisation effects easy to observe. The interest comes from a fundamental point of view, several novel and surprising effects have already been discovered, as well as from an application point of view. In the latter case the hope is that mesoscopic-, or even nano-objects, shall be useful for further miniaturisation of devices and circuits.

In this paper we will describe some of our recent investigations of the behaviour of electrons in different quantum confined systems. First, we will review our studies of band structure parameters, and in particular the effective spin-splitting factors, in low dimensional structures. We will continue by describing our first results on magneto- optical investigations of quantum dot systems. This will be followed by a description of our investigations of the magnetoresistance of 2D- and 1D-channels where the ballistic electron motion is perturbed by randomly deposited aerosol particles. These nano-particles are either metallic or superconducting, with well defined diameters between 30 - 300 nm. We will, finally, present studies of a 1D switching device, the Y-branch switch, where mode evolution rather than quantum interference effects are used.

II. Band structure parameters in low dimensional systems

The band structure is well known for most common bulk semiconductors, but for low-dimensional structures such as quantum wells, quantum wires and quantum dots, the details are still not understood. The aim is to understand the band structure of low- dimensional systems to such a precision, that theoretical modelling of arbitrary materials and geometries can be performed. In order to realise this, fundamental parameters have to be measured and understood. A band structure parameter representing a high degree of precision is the effective spin splitting factor, g^*. This effective spin splitting can be calculated within most theoretical models. Accurate experimental determination of g^* is, therefore, of fundamental importance in solid state physics since it provides a sensitive test of band structure calculations and theoretical concepts in general[2-4].

The experimental work[5-7] was performed on p-modulation doped $Ga_xIn_{1-x}As$ single quantum well (SQW) and multiple single quantum wells (MQW) grown by metal organic vapour phase epitaxy (MOVPE) either lattice-matched (x_{Ga}=0.47) to InP having different well thicknesses, or with varying composition ($0.4 < x_{Ga} < 0.6$) but fixed QW thickness (d=15 nm). For further details see Ref. 5.

The optically detected resonance (ODMR) experiments were performed at 24 GHz using a 4T mag-

net system. For the resonance experiments the circularly polarized components of the photoluminescence (PL) emission in Faraday configuration were analyzed by a combination of linear polarizers and a photo-elastic stress modulator.

A PL spectrum from a d=15 nm $Ga_{0.47}In_{0.53}As$/InP QW shows a single line at 0.83 eV with a half width of 8 meV[6]. The line is due to band to band recombination between the first electron and heavy hole subband (e_1hh_1). The emission is circularly polarized (magnetic circular polarized emission, MCPE) with the degree of polarization depending on temperature and the applied magnetic field. This behaviour is caused by an unequal spin population in the Zeeman split states and is a necessary condition to perform magnetic resonance experiments. The difference in occupation is changed by resonant microwaves, and the magnetic resonance signal is observed as a change of the MCPE signal (see Fig. 1). Using the resonant magnetic field B_{res} and the constant microwave energy $\Delta E_{\mu w}$ the g^* values were calculated in the spin S=1/2 formalism by the relation

$$\Delta E_{\mu w} = g^* \mu_B B_{res} \qquad (1)$$

where μ_B is the Bohr magneton. For this particular sample, and for the magnetic field parallel to the QW growth axis we obtain a g^*-value of $g_\parallel = -3.27 \pm 0.04$. When rotating the sample from the $< 001 >$ towards an in-plane direction [011], the g^*-value decreases significantly. The g^*-value was determined from the standard expression for a g-tensor in axial symmetry

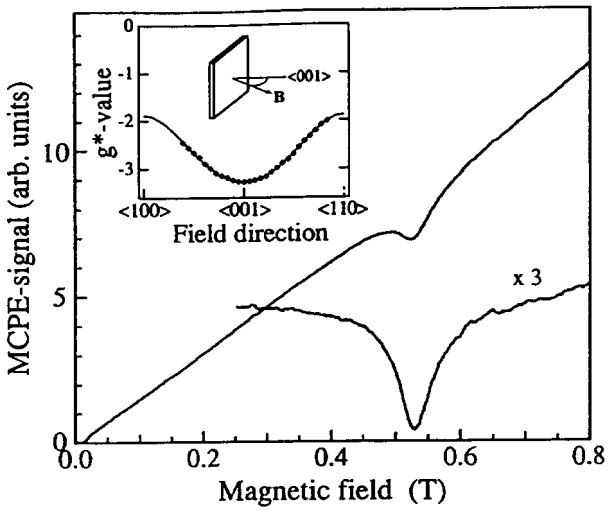

Figure 1. ODMR detected on the magnetic circular polarized emission (MCPE) signal of a 15 nm single $Ga_{0.47}In_{0.53}As$/InP QW at T= 1.6 K. From Ref. 5.

$$g^*(\theta) = (g_\parallel^2 \cos^2\theta + g_\perp^2 \sin^2\theta)^{1/2} \qquad (2)$$

where θ is the angle between the magnetic field and the quantum well plane. The solid line in Fig. 2 is the result when using $g_\perp = -1.88 \pm 0.04$.

Alternating the QW width at constant alloy composition ($x_{Ga} = 0.47$) changes the g^*- values as well as the $g_\parallel/g_\perp$ ratio (Fig. 2). In the quasi-3D case (d=100 nm) a $g^* = -4.01 \pm 0.04$ resonance is obtained, which is isotropic within the experimental uncertainty. With increasing quantisation (decreasing QW width) the anisotropy increases to $g_\parallel/g_\perp = 4$ for d=6 nm, the thinnest QW for which ODMR could be observed. The strained samples with different compositions in the QW (d= 15 nm) showed substantial changes of the $g_\parallel$- and the $g_\perp$-values. Both $g_\parallel$ and $g_\perp$ increase approximately linearly with Ga content in the investigated composition range, but the anisotropy ratio $g_\parallel/g_\perp$ remains almost constant.

It can be shown that only the population difference within the electron Kramers doublet gives rise to circular polarization of the PL, and that the spin resonances take place at the edge of the lowest conduction subband[5–7]. A prerequisite to observe ODMR is the introduction of spin transitions within the life-time of the decaying system. For the standard cw-ODMR technique, life-times must be longer than $\approx 0.1\mu$s. Therefore, it is not surprising that the few, existing experimental results are obtained on type-II QW' s or super lattices[8–11]. Here the electrons and holes are separated in real space. This separation of the carriers leads to recombination times in the microsecond range. The observation of spin resonance signals in our type-I QW structures is, therefore, apparently facilitated by the spatial separation of the electron and hole wave-functions caused by the one-sided modulation doping. Investigations of the PL lifetimes show, however, that the increase of the lifetimes is too small to explain the results. Another possible reason may be the admixture of p-type states in the pure spin-up and spin-down s-type wave-functions of the conduction band due to the electric field, $\mathbf{k} \cdot \mathbf{p}$ interaction and inversion asymmetry[12]. This could, in principle, lead to a relaxation of the pure magnetic dipole selection rules

and an increased spin-flip probability through electric dipole spin transitions.

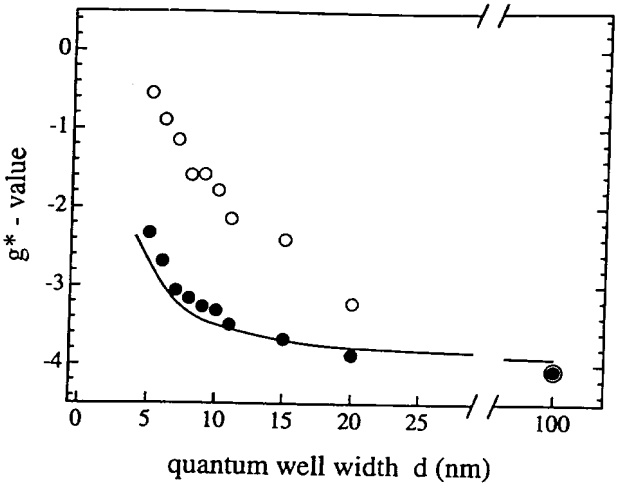

Figure 2. $g_{\parallel}$ (solid circles) and $g_{\perp}$ (open circles) for different well widths in $Ga_{0.47}In_{0.53}As/InP$ QW's. The solid line is the result of a calculation (see Ref. 5).

These data give an experimental proof of quantum confinement-dependent anisotropy of g^* as predicted by Ivchenko and Kiselev[4]. A calculation of the $g_{\parallel}$-values as a function of QW width for the unstrained $Ga_{0.47}In_{0.53}As/InP$ system[5] leads to quantitatively good agreement with experimental data (see Fig. 2). It is, however, a difficult task to calculate the $g_{\perp}$-value, since an accurate choice of basis functions is non-trivial.

The calculation of $g_{\parallel}$-values in the case of d=15 nm QW's with varying alloy composition is in principle possible, but at present the information regarding interband coupling terms in the case of compressive and tensile strain is not available. The calculation of $g_{\parallel}$, including electric field-, quantum confinement-, and strain-effects, approximating the interband coupling terms from a linear interpolation between the lattice-matched $Ga_{0.47}In_{0.53}As$ and the binaries, is in reasonable agreement for higher x_{Ga}-values, but deviates for smaller x_{Ga}-values[5]. The calculation of the $g_{\perp}$-value is, for the above-mentioned reasons, even more difficult in this case.

III. Magneto-optics of quantum dot systems

The possibilities to create semiconductor structures where the electron motion is restricted in all three dimensions have received considerable attention during the last years. Strained quantum dots formed during morphological transition from two dimensional layer by layer growth to three dimensional Stranski-Krastanov[13] island growth is one of the promising techniques to form such quantum dots[14]. The resulting embedded islands have electronic properties with 3D confinement defined by ideal heterointerfaces. This gives opportunities to study the physical properties of these zero- dimensional objects. Here we will describe some results from studies of the exchange interaction of excitons confined in such quantum dot systems[15].

InAs islands embedded in GaAs were grown by chemical beam epitaxy (CBE). After a growth of 2 monolayers of InAs and a growth interrupt a steady state 3D island nucleation was observed using reflection high energy electron diffraction (RHEED). The approximate height and diameter of the InAs islands are 3 nm and 12 nm, respectively.

The PL spectrum shows a broad (FWHM $\approx$ 100 meV) peak at 1.24 eV which is attributed to InAs islands with a slight size variation. Because of the strain and confinement situation in the dot the PL feature is assigned to the exciton transition between electron and heavy hole states in the islands. Under the influence of a magnetic field the Hamiltonian describing the states is given by

$$H_{\text{exciton}} = H_e + H_{hh} + H_{\text{exchange}} \qquad (3)$$

representing the Zeeman interaction of electrons, heavy holes and the exchange interaction, respectively. The energies of the four eigenstates evolve in a magnetic field as schematically shown in Fig. 3. Δ is the exchange constant introducing a splitting of the spin parallel and antiparallel pairs of states. The states are denoted by the hole and electron spin directions $|\pm,\pm>$. Of those only the two $|\pm,\mp>$ are optically allowed and emit circularly polarized photons. At certain magnetic field values the optically allowed states cross the optically inactive states. These fields are

$$B_{LC,h} = \Delta/(\mu_B g_{hh}) \qquad (4)$$

$$B_{LC,e} = \Delta/(\mu_B g_e) \qquad (4)$$

where LC denotes level crossing.

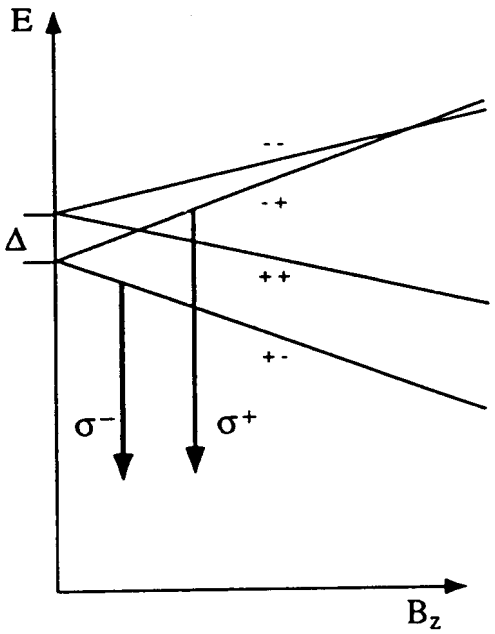

Figure 3. Schematic excitonic level diagram in the presence of a magnetic field.

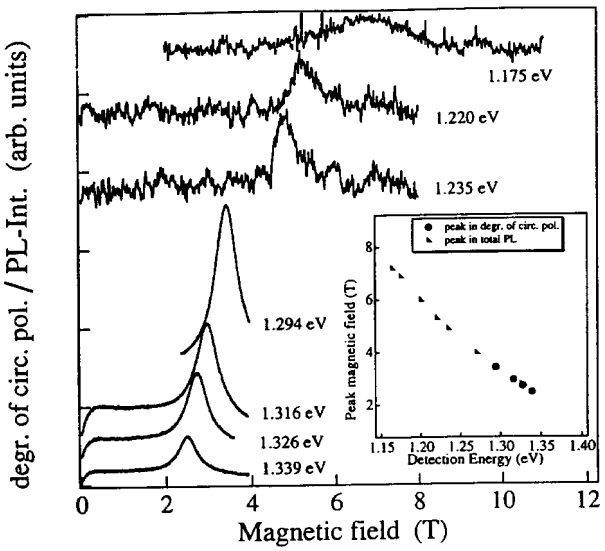

Figure 4. A collection of $\sigma^- - \sigma^+$ traces, as well as PL (the three upper curves) intensity as a function of magnetic field. The inset shows the resulting peak magnetic fields as a function of detection energy within the PL peak.

When applying a magnetic field using a constant detection energy, a circular polarization $P = (\sigma^-\sigma^+)$ was observed (Fig. 4). At specific magnetic fields a pronounced increase of the signal was found, the field position depends on the detection energy. The peak shifted to higher magnetic field as the detection energy was reduced.

The experimental results can be understood in the following model. Our excitation generates heavy hole excitons in all four states. The population in the levels split by the magnetic field thermalizes, the exact distribution depends on spin relaxation and radiative recombination times. It is, however, only the optically allowed levels that contribute to the PL signal. At the level crossings the optically allowed levels are fed by the inactive levels, leading to an increase of the σ^- and σ^+ components, respectively, at the two level crossing fields. We identify the experimentally observed increase of the σ^- component to the level crossing at $B_{LC,h}$. We could not detect the second level crossing in the available fields range $\leq 18T$. This might be expected since the coupling is smeared out over a large magnetic field (see Fig. 3) and might be difficult to detect.

Individual InAs dots with different size and shape variations luminesce at different energies. Therefore, the dependence of $B_{LC,h}$ on detection energy within the island PL peak gives direct information of the exciton exchange interaction as a function of the dot size[16]. As can be seen in Eq. 4, Δ and g_{hh} influence the position of the level crossing. It is known that both parameters can be influenced by quantum confinement, and, therefore, two explanations for the observed behaviour can be given[15]. Here we will only recapitulate one, the reduced exchange interaction energy Δ due to a large leak out of the envelope function into the barrier. Theoretical studies show that with increasing quantum confinement the electron wave function will leak out into the surrounding GaAs barrier. The heavy hole state is, however, not affected as drastically due to its larger effective mass. The result is a smaller overlap of the wave functions for smaller dot sizes, leading to smaller Δ and lower $B_{LC,h}$ in agreement with the experimental observations. Even though the g_{hh} is unknown, we can estimate the exchange interaction as a function of dot size by using Eq. 4 and the extreme values of the g-values of InAs and GaAs. The result is presented in Fig. 5. As the dot size we have used half the base size of the dot. It should be noted that the quantisation effect on the g_{hh} values is not considered here. For comparison, the exchange energies in AlGaAs/GaAs QW's are typically one to two orders of magnitude smaller.

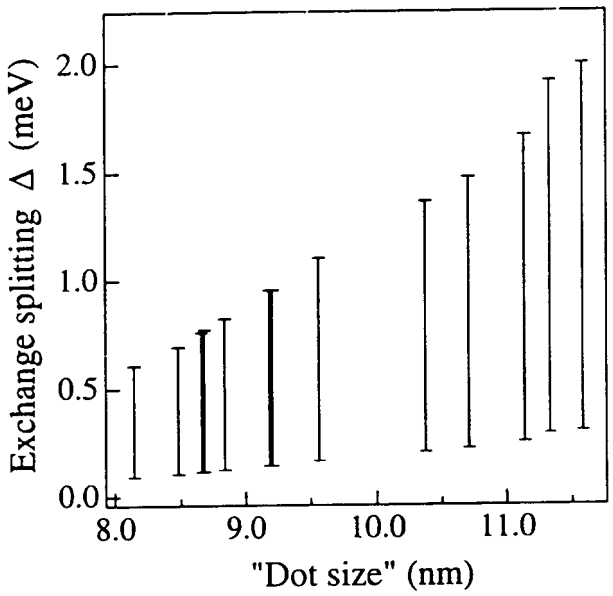

Figure 5. Estimates of the excitonic exchange splitting as a function of dot size.

IV. Magnetotransport of perturbed 2D- and 1D-channels

For the study of ballistic transport and quantum interference effects such as the ballistic point contact[17], the Weiss oscillations[18] and the Aharonov-Bohm effect[19], a laterally perturbed two-dimensional electron gas (2DEG) in a modulation-doped GaAs/AlGaAs structure is often used. Restrictions and modulations of the potential landscape are usually established by electrical potentials created by etching or gating techniques. Recently, inhomogeneous magnetic fields have also been used as a tool to influence the movement of electrons[20–23]. Most techniques require photo- or electron- beam-lithography techniques to obtain the desired patterning of the sample. Another approach to obtain electric or magnetic potential variations is to randomly place metal particles on top of a 2DEG sample. Electric potential variations due to a change of the surface states at the location of the particles or due to thermal stress can be anticipated. The typical length scale of the modulation is then given by the grain size and the particle density. We have carried out such experiments using 33 nm large silver particles on top of a 2DEG, which resulted in an increase of the mobility of the 2DEG[24].

If superconducting particles are used, they are expected to expel an external magnetic field due to the Meissner effect, and thus create magnetic inhomogeneities in the plane of the 2DEG. This has been demonstrated using type-I superconducting lead powder[23–25]. Here we describe some further observations when reducing the size of the lead particles and their average separation, even to well below the mean free path of the electrons.

The samples were standard Hall bars 50 μm wide and with 100 μm distance between the voltage probes. They were fabricated from a modulation-doped GaAs/AlGaAs heterostructure containing a 2DEG with carrier density 2×10^{15} m^{-2}, mobility 130 m^2/Vs and a mean free path $\approx 9\mu$m. We carried out standard ac magnetoresistance experiments using a typical rms current of 50 nA at T = 300 mK.

If lead powder with grain sizes as small as 5 μm in diameter is deposited on top of the sample a magnetoresistance with a pronounced structure was found[25]. Upon application of a magnetic field the Meissner effect of the lead expels the magnetic field and produces an inhomogeneous magnetic field in the 2DEG, causing enhanced magnetoresistance ($\approx$ 3 %). The peaks disappeared at the critical temperature and the critical field, for lead respectively $T_c = 7.2$K and $B_c = 0.08$ T. A hysteresis due to the frozen intermediate state in the lead grains was also observed. Classical transport theory was applied and good agreement with the theory of Smith and Hedegård[26] was found.

To further reduce the size of the lead particles, we have used an aerosol technique as described in Ref. [27]. Spherical aerosol particles of very homogeneous size distribution are deposited over the entire Hall bar (Fig. 6). Particle sizes used were between 80 nm and 300 nm, at densities between 0.02 μm^{-2} and about 0.6 μm^{-2}. The diameter of the particles is thus in all cases much smaller than the electron mean free path, while the typical distance between two lead particles was varied above and below the mean free path.

In all samples with lead lead particles particles, except for the sample with the lowest particle density, we observe a small symmetric peak of the magnetoresistance ($\Delta R/R \approx 0.5\%$) at zero magnetic field. The peak is of Lorentzian shape with a full width at half maximum (FWHM) of about 20 mT. With increasing temperature the peak is reduced and disappears

at about 5 K. In width and shape the feature does not resemble the commonly observed weak localization peak. It should be noted that occasionally a very similar peak has also been observed in samples treated in ways not involving superconducting particles. The origin of this resistance peak is not understood at present. For reasons presented in Ref. 25, we conclude that our spherical particles, with $d \leq 300$ nm, probably do not cause magnetic inhomogeneities in the plane of the 2DEG. One reason could be that the magnetic screening of the particles is too small in scale and strength compared to their distance to the 2DEG. The mobility and the carrier concentration of the samples were not changed significantly in the presence of the lead particles, but at particle densities higher than about 0.1 μm^{-2}, the single-particle relaxation time, as deduced from the Shubnikov-de Haas (SdH) effect, was reduced by about 20%. Consequently, the particles cause only very weak electrical potential modulations leading to small-angle scattering.

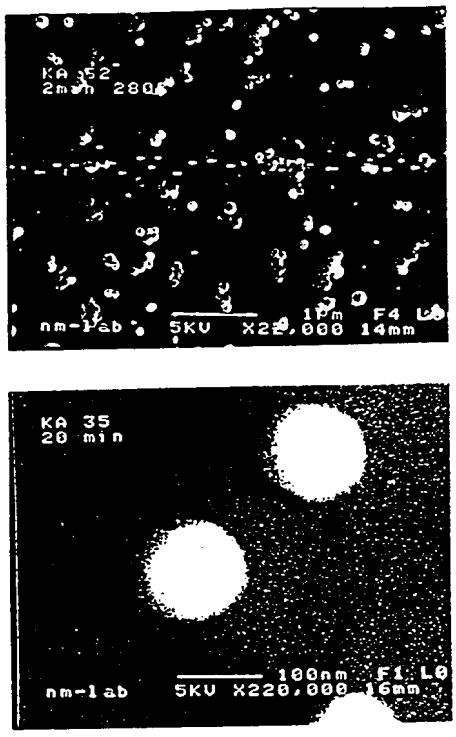

Figure 6. Spherical shaped, homogeneous sized (0.6 μm^{-2}) of 110 nm diameter on a GaAs surface. From Ref. [25].

Melting the lead particles at 370°C in a nitrogen atmosphere resulted in drastic changes. Whereas a reference sample without lead did not change at all upon heat treatment, the zero-magnetic-field resistance of a sample with lead increased by a factor of 6, and the carrier concentration was reduced by about 15%. A strong, Lorentzian negative magnetoresistance appeared, reducing the resistance at B = 0.2 T to 50% of the value at B = 0. For samples with different particle densities we found that the FWHM of the Lorentzian magnetoresistance decreases with increasing density. We found also that the widths of the quantum Hall plateaus of the heated samples systematically increased with particle density, up to a relative change of 60%. Clearly, the melted lead particles introduce a strong potential variation in the 2DEG. At zero field a maximum of magnetoresistance was observed, which seems to consist of two contributions: one narrow, sharp peak of about 2mT due to increased weak localization caused by the additional scatterers, and an underlying broader contribution very similar in shape, relative size and temperature dependence to the feature we observe in the lead-containing samples before heating[25].

To increase the effects of the lead particles, we used a narrow channel defined by shallow wet etching in a 30 m^2/Vs GaAs/AlGaAs sample[25]. The lithographic width and length of the channel were 400 nm and 5 μm, respectively. In Fig. 7 (bottom trace), the magnetoresistance of a channel without particles is shown. Reproducible, aperiodic conductance fluctuations, and an underlying magnetoresistance with a maximum at B = 0.22 T is observed. This is a classical magneto size effect due to diffusive scattering at the edges of the channel. From the location of the maximum we estimate the effective width of the channel to he 250 nm.[28]

Lead particles with a size distribution between 80 and 250 nm were randomly distributed on the structure (see inset, Fig. 7). The magnetoresistance changed significantly (Fig. 7, top trace). The zero-magnetic-field resistance is about 50% higher than before particle deposition, and the maximum of the magnetoresistance at $|B| \approx 0.2$ T has disappeared. These changes are probably a result of changes in the potential landscape in the channel caused by the deposited particles which introduce a varying channel width. The magneto size effect leading to a well defined maximum is then obliterated.

The sharp maximum at B = 0 T has increased from $\Delta G = 0.4e^2/h$ to about 0.6 e$^2/h$. We attribute this peak to impurities in the channel causing coherent backscat-

tering which is suppressed by the magnetic field. Such an effect should be enhanced when more scatterers are introduced into the channel. Another indication that this is a quantum interference effect is the temperature dependence of the resistance between 0.3 and 5 K. Whereas the resistance, averaged over some conductance fluctuations, *increases* with temperature before particle deposition, it *decreases* afterwards.

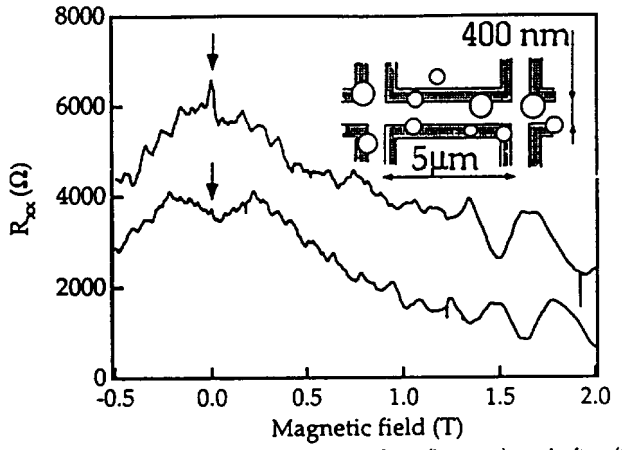

Figure 7. Magnetoresistance of a quasi-1D channel before (bottom) and after (top) lead particle deposition. The inset show the positions of the particles. Arrows indicate the position of the sharp peaks at B= O T. From Ref. 25.

V. A 1D switching device

Several device concepts based on the physics of one-dimensional (1D) electron waveguide structures have been suggested. In such concepts ballistic phase coherent electron transport is used instead of drift and diffusion of the carriers. There have been suggestions of, for instance, Aharonov-Bohm type devices[29,30], directional couplers[31,32] as well as a quantum stub transistor[33]. The operation of these devices is based on a conductance which oscillates when an applied gate voltage, or magnetic field, is changed. The extreme sensitivity to fabrication imperfections and background charge from impurities has put forward doubts about the realism of such devices[34]. Another principle, based on modal evolution rather than interference of 1D-electrons, was recently suggested[35–37]. The idea was brought from the field of optics[38], where it is well known that an integrated optics Y-branch switch, or digital switch, possesses several advantages compared to interferometrics witches[39]. An analysis of the electron-wave Y-branch switch showed that a wider electron velocity spectrum than for interferometric devices is allowed and that the Y-branch switch does not require single-mode electron waveguides[36], although switching voltages will be increased for multi-mode devices. The latter is of considerable importance for high temperature operation possibilities.

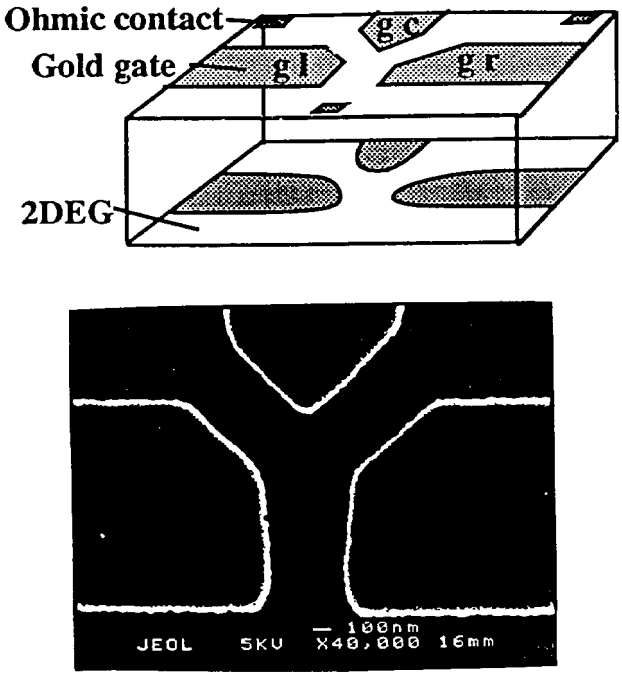

Figure 8. Schematic picture of the Y-structure defined by Schottky gates (top) and a SEM picture of the real structure (bottom).

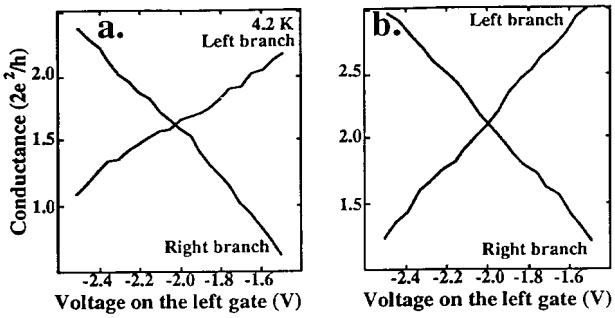

Figure 9. Experimental (left) and calculated (T=OK) conductance through the two branches of the Y-branch switch as a function of the applied perpendicular voltage. The sum of the voltages on the left and the right side is kept constant.From Ref. 41.

Here we describe our experimental realisation of the Y-branch switch[40,41]. The samples were fabricated from modulation-doped AlGaAs/GaAs heterojunctions containing a two dimensional electron gas (2DEG) with mobilities $\mu = 1 - 3 \times 10^5$ cm^2/(Vs) and

$N_{2D} = 4 - 7 \times 10^{11}$ cm^{-2} at 4.2 K. The devices are defined using electron-beam lithography[42] and a lift-off procedure. Negatively biased Schottky-gates are used for the definition of the Y-structures (Fig. 8). The samples have lithographically defined widths of 200 - 400 nm, a length of about 1.3 μm and a branching angle of 90°. By changing the negative bias on the Schottky-gates, and thereby the extension of the depletion region under the gates, it is possible to change the width of the waveguide from approximately the lithographically defined down to zero. During the branching experiments the widths of the waveguides in the 2DEG is in the order of the Fermi-wavelength, and the electrons can no longer be treated classically, rather as quantum-mechanical particles or waves.

The devices have been measured in constant voltage mode. The transverse field is created by lowering the potential on one sidegate and increasing it on the other. The currents are measured simultaneously in the two branches. The three split gates can be individually biased. The voltage on the central gate, g_c in Fig. 8, is kept constant while the bias on the left and the right gates, g_l and g_r in Fig. 8, is varied during measurement. By keeping the sum of the voltages on the left and the right gate constant, a certain number of current modes will enter the device, assuming we have 1D-transport. The one-dimensional character of the transport is verified by a two probe measurement of the quantised conductance[43,44].

The branching properties of the samples have been measured both at 4.2 K and 77 K. The current switching ratio is about 4:1 at 4.2 K (Fig. 9) and decreases to about 2:1 at 77 K. An overall decrease of the conductance at 77 K is also observed. This is probably due to increased thermal scattering and the loss of ballistic transport in the constriction. There is also quite a large variation in the performance of devices fabricated in an identical way.

The experimental results have been compared with a semiclassical calculation and a good agreement between experiments and theory is found (see Fig. 9). Despite this good agreement, it is not unambiguously proven, so far, that the device is working as an electron-wave branching device. The drawback with the gate electrode approximation of the structure is that the switching field has to be applied between the left and the right gate electrodes. An inherent disadvantage with this is that the applied bias voltage moves the waveguides in addition to producing the electric field required for switching. This also means that an increased voltage is needed for switching.

The operation of this device appears to be similar to having a FET at each drain branch. The principle of operation is, however, different, and it can be shown that, for a single-mode device, a Y-branch switch can have a lower switching voltage than a FET[37]. For multi-mode devices one will approach the classical behaviour of a FET. Detection of true mode-evolution is therefore not straight forward.

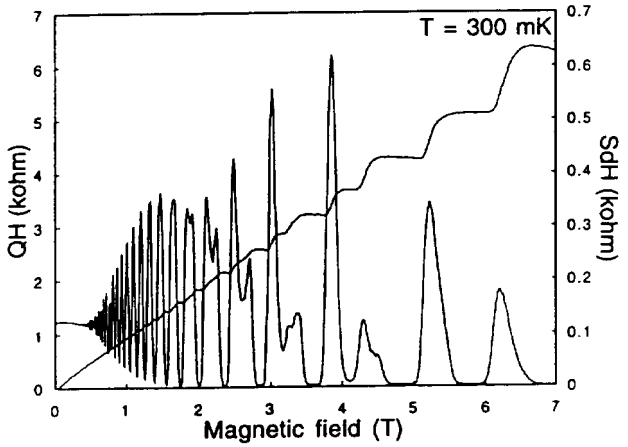

Figure 10. Quantum Hall- and SdH-data of a high mobility $Ga_{0.25}In_{0.75}As/InP$ 2DEG sample. The mobility is 466 000 cm^2/Vs.

To overcome some of the above mentioned problems we have produced high mobility $Ga_{0.25}In_{0.75}As/InP$ 2DEG samples with mobilities exceeding 450 000 cm^2/Vs.[45] Fig. 10 shows the quantum Hall and the Shubnikov-de Haas data of one of these samples which is terminated with an epitaxially grown Schottky gate. Etching procedures and epitaxial regrowth are then attempted with the goal of defining Y-branch structures by epitaxial growth. Among the advantages with this concept, the increased quantisation, and thereby the possibilities of high temperature device operation, can be mentioned.

Acknowledgements

These works have been performed within the nm-structure consortium in Lund and financed by the Swedish Natural Science Research Council, the Swedish

Research Council for Engineering Sciences and by NUTEK.

References

1. See e.g. *Nanostructure Physics and Fabrication*, Eds. M. A. Reed and W. P. Kirk, (Academic Press, 1989).
2. U. Rössler, F. Malcher and G. Lommer, Springer Series in Sol. State. Science, Vol. 87, Ed. by G. Landwehr (Springer Verlag, Berlin, 1989) p. 376.
3. G. Hendorfer and J. Schneider, Semicond. Sci. Technol. **6**, 595 (1991)
4. E. L. Ivchenko and A. A. Kiselev, Sov. Phys. Semicond. **26**, 827 (1992) [Fiz. Tekh. Poluprovodn **26**, 1471 (1992)].
5. B. Kowalski, P. Omling, B. K. Meyer, D. M. Hofmann, C. Wetzel, V. Harle, F. Scholz and P. Sobkowicz, Phys. Rev. B**49**, 14786 (1994).
6. P. Omling, B. Kowalski, B.K. Meyer, D.M. Hofmann, C. Wetzel, V. Harle, and F. Scholz, Solid-State Electronics **4-6**, 669 (1994).
7. B. Kowalski, P. Omling, B.K. Meyer, D.M. Hofmann, V. Harle and F. Scholz, Physica Scripta T**54**, 100 (1994).
8. H. W. van Kesteren, E. C. Cosman, F.J.A.M. Greidanus, P. Dawson, K.J. Moore and C.T. Foxon, Phys. Rev. Lett. **61**, 129 (1988).
9. E. Glaser, J. M. Trombetta, T. A. Kennedy, S. M. Prokes, D. J. Glembocki, K. L. Wang and C. H. Chern, Phys. Rev. Lett. **65**, 1247 (1990).
10. J. M. Trombetta, T. A. Kennedy, D. Gammon and S. M. Prokes, in "20th Int. Conf. on Semicond. Phys.", ed. by E.M. Anastassakis and J.M. Joannopolos, (World Scientific, Singapore, 1990) p. 1361.
11. E. R. Glaser, T. A. Kennedy, D. J. Godbey, P. E. Thompson, K. L. Wang and C.H. Chern, Phys. Rev. B**47**, 1305 (1993).
12. M. Brown and U. Rossler, J. Phys. C: Solid State Phys. **18**, 3365 (1985).
13. I. N. Stranski and L. V. Krastanov, Akad. Wiss. Let. Mainz Math. Natur. Kl. IIb **146**, 797 (1939).
14. J. Y Marzin, J. M. Gerard, A. Izrael, D. Barrier and G. Bastard, Phys. Rev. Lett. **73**, 716 (1994).
15. B. Kowalski, P. Omling, M.S. Miller, S. Jeppesen and L. Samuelson, Proceedings "Modulated Semiconductor Structures-7", Madrid (1995).
16. J.Y. Marzin and G. Bastard, Solid State Commun. **92**, 437 (1994).
17. B.J. van Wees, H. van Houten, C.W.J. Beenakker, J.G. Williamson, L.P. Kouwenhoven, D. van der Marel and C.T. Foxon, Phys. Rev. Lett.**60**, 848 (1988).
18. D. Weiss, K. von Klitzing, K. Ploog and G. Weimann, Europhys. Lett. **8**, 179 (1989).
19. G. Timp, A.M. Chang, J.E. Cunningham, T.Y. Chang, P. Mankiewich, R.E. Behringer and E. Howard; Phys. Rev. Lett. **58**, 2814 (1987).
20. A.K. Geim; Pis'ma Zh. Eksp. Teor. Fiz. **50**, 359 (1989). [JETP Lett. **50**, 389 (1989)].
21. S.J. Bending, K. von Klitzing and K. Ploog; Phys. Rev. Lett. **65**, 1060 (1990).
22. A. K. Geim, S.J. Bending and I.V. Grigorieva; Phys. Rev. Lett. **69**, 2252 (1992).
23. A. Smith, R. Taboryski, L. Theil Hansen, C.B. Sørensen, P. Hedegård and P.E. Lindelof; Phys. Rev. B**50**, 14726 (1994).
24. P. Omling, H. Linke, K. Deppert, L. Samuelson, H.A. Carmona, A.K. Geim and P.C. Main; Superlatt. Microstruct. 15, 367 (1994).
25. P. Omling, H. Linke, K. Deppert, L. Samuelson, L. Theil Hansen, and P.E. Lindelof; Japan. J. of Appl. Phys. **34**, 4575 (1995).
26. A. Smith and P. Hedegard, Phys. Rev. B in press (1995).
27. K. Deppert, H.-C. Hansson, I. Maximov, L. Samuelson and A. Wiedensohler; Appl. Phys. Lett.**64**, 3293 (1994).
28. C.W.J. Beenakker and H. van Houten; Sol. St. Phys. 44, eds. H. Ehrenreich and D. Turnbull (Academic Press, Boston, 1991).
29. S. Bandyopadhyay, S. Datta and M.R. Melloch, Superlatt. and Microstruct. **2**, 539 (1986).
30. S. Bandyopadhyay and W. Porod, Appl. Phys. Lett. **53**, 2323 (1988).
31. J. A. del Alamo and C. C. Eugster, Appl. Phys. Lett. **56**, 78 (1990).
32. N. Tsukada, A. D. Wieck, and K. Ploog, Appl. Phys. Lett. **56**, 2527 (1990).
33. F. Sols, M. Macucci, U. Ravaioli and K. Hess, J.

Appl. Phys. **66**, 3892 (1989).
34. R. Landauer, Physica A **168**, 75 (1990).
35. T. Palm and L. Thylén, Appl. Phys. Lett. **60**, 237 (1992).
36. T. Palm, J.Appl. Phys. **74**, 3551 (1993).
37. T. Palm, L. Thylén, O. Nilsson and C. Svensson, J. Appl. Phys. **74**, 687 (1993).
38. W. K. Bums, A. B. Lee and A. F. Milton, Appl. Phys. Lett. **29**, 790 (1976)
39. Y. Silberberg, P. Perlmutter and J. E. Baran, Appl. Phys. Lett. **51**, 1230 (1987).
40. P. Ramvall, P. Omling, T. Palm and L. Thylén, Quantum Confinement: Physics and Applications, p. 76 (The Electrochemical Soc, 1994).
41. P. Omling, P. Ramvall, T. Palm and L. Thylén, Proceedings of the 22nd International Conference on the Physics of Semiconductors, Ed. D.J. Lockwood (World Scientific Publishing, Singapore, 1995) p. 1649.
42. M. J. Rooks, C.C. Eugster, J. A. del Alamo, G. L. Snider and E. L. Hu, J. Vac. Sci. Technol. B**9**, 2856 (1991).
43. B. J. van Wees, H. van Houten; C. W. J. Beenakker, J. G. Williamson, L. Kouwenhoven, D. van der Marel and C. Foxon, Phys. Rev. Lett. **60**, 848 (1988).
44. D. A. Wharam, T. J. Thornton, R. Newbury, M. Pepper, H. Ahmed, J. E. Frost, D. G. Hasko, D. Peacock, D. Ritchie and G. Jones, J. Phys. C**21**, L209 (1988).
45. N. Carlsson, W. Seifert, P. Rarnvall, S. Anand, Q. Wang, M. Stoltze, P. Omling and L. Samuelson, "Proceedings European Workshop on MOVPE", Gent (1995).